International Research Journal of Engineering and Technology (IRJET) e-ISSN: 2395-0056
Volume: 11 Issue: 10 | Oct 2024 www.irjet.net p-ISSN: 2395-0072

Study of the mechanical behavior of the dual mobility hip joint in different activities of the patient.

Le Thi Bich Nam

School of Mechanical Engineering, Hanoi University of Science and Technology,
No.1 Dai Co Viet Road, Hanoi, Vietnam

---***---

Abstract - *Previous studies on the mechanical behavior of artificial hip joints have focused on standard joints, which only allowed the movement of the head in the liner. The finite element method was used to investigate a part of the joint assembly in different patient activities. In this study, the finite element method was effectively used to investigate the mechanical behavior of the dual mobility hip joint, which is a type of joint that allows for more extensive joint degree movements. The mechanical behaviors investigated include the equivalent Von-Mises stress, the total deformation, the total displacement, the contact pressure, and the sliding distance in human activities such as daily walking and difficult positions such as sitting on a chair or sitting on the floor. Additionally, the materials used to manufacture hip joints have been expanded to include biomaterial with strength equivalent to human bones, such as CF-PEEK plastic, in addition to materials commonly used for hip joints such as Cobalt-Chrome, Titanium, etc.*

Key Words: Artificial hip joint, Implant, Human activities, Mechanical behaviour of AHJ, Sliding distance, Finite element method, Biomaterial …

1.INTRODUCTION

The hip joint plays a crucial role in supporting the body's weight during daily activities, connecting the lower limbs to the spine, and transmitting force from the ground to the top. The need for artificial hip joint (AHJ) replacement is increasing, with elderly individuals suffering from joint disease or deformities, as well as younger individuals due to vigorous activities or accidents. The main reasons for hip replacement include osteoarthritis, fractures, and changes in bone structure and connective tissue, leading to loss of motor function and pain.

After hip replacement surgery, issues such as joint slippage, friction between joint parts causing wear, and the release of metal particles into the body need to be considered. Additionally, the durability and longevity of the artificial joint during the patient's activities and overtime are important factors. Previous studies have used metallic materials for hip joints, but these have drawbacks such as incompatibility with the human body and obstruction in X-rays. To address these issues, the use of plastics like HDPE for the Liner and PEEK for the Stem and Cup of artificial hip joints has been explored. These materials offer biocompatibility and transparency in X-rays or CT scans, allowing for more accurate assessments. When PEEK is reinforced with carbon fiber, it can match the strength and stiffness of natural human bone, preventing stress imbalance with surrounding bone and ensuring even force distribution. Stem made from PEEK material to increase the bond with bone, it is necessary to use more bio-cement or add HA coating by Plasma coating method. Nowadays, PEEK-CF material is gradually replacing Titanium in its applications [5]. In this research, parts of AHJ made of metal (Coban-chrome, Titanium) and CF-PEEK are investigated.

The finite element method (FEM) is an essential mechanical analysis method used to evaluate mechanical behaviour of the artificial hip joint. It is used to simulate the effects of motion and loading on artificial joints. Al-Shammari [9] used FEM to study a standard hip joint model, investigating different angles of the stem to find the optimal angles of implants, and investigating the mechanical behaviour of AHJ made of aluminium and CoCr alloy materials in the normal walking posture of the patient. Eko Saputraa et al. [3] also used FEM to investigate the stress in the Liner and Head assembly in different sitting postures of the patient including sitting on a chair, squatting, kneeling, and bowing.

Previous studies have mainly focused on standard hip joints or only examined specific parts of the hip assembly [9], such as the contact between the liner and the head, or the cup-liner contact [3]. This study extends the investigation of mechanical behaviour to the dual mobility hip joint, a type of hip designed to spread motion angles. The dual mobility hip allows two motions: the Head can move in the Liner and the Liner can move in the acetabular Cup. As a result, this implant has the potential to reduce the risk of dislocation and improve joint stability, making it suitable for younger patients with a wide range of movements. Most of the patient's movement postures in daily life were surveyed, including standing, sitting on chairs, and sitting on the ground. The mechanical behaviours that were studied included stress distribution, deformation distribution, and displacement distribution on the joint details. Additionally, the study also examined the contact pressure and sliding distance between the articulating parts.

International Research Journal of Engineering and Technology (IRJET) e-ISSN: 2395-0056
Volume: 11 Issue: 10 | Oct 2024 www.irjet.net p-ISSN: 2395-0072

2. MODELING AND METHOD

1.1 Modeling and material

The dual mobility artificial hip joint consists of four parts: the Cup, Liner, Head, and Stem (refer to Fig. 1). The geometry dimensions can be found in Table 1, and the angle of the Stem is 50 degrees. The artificial hip joint is made of two groups of materials as shown in Table 2, with the property parameters of the materials outlined in Table 3. The geometry dimensions in Table 1, the angle of the Stem is 50 degrees. The AHJ is made of two groups of materials shown in Table 2, with property parameters of materials in Table 3.

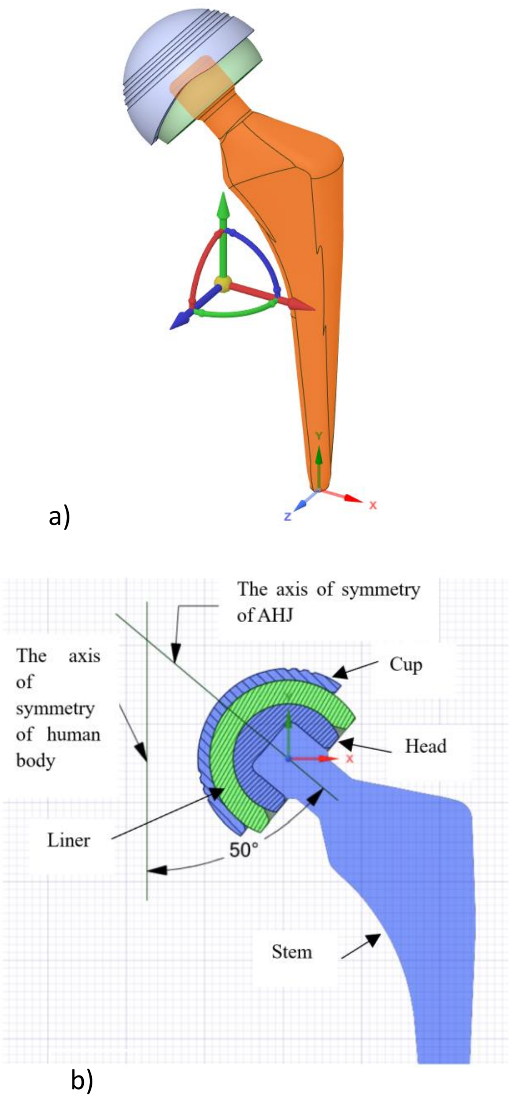

Figure -1: The dual mobility hip joint modeling

Table -1: Geometry parameters of the artificial hip joint

Cup	Inner diameter	40 mm
	Outer diameter	46 mm
Liner	Inner diameter	40 mm
	Outer diameter	28 mm
Head	Inner diameter	28 mm
	Outer diameter	16 mm
Stem	Stem Length	99 mm
	Neck length	35 mm
	Distal diameter	8mm

Table 2: Materials made of the hip joint

Material groups	Cup	Liner	Stem	Head
Material 1	Coban – Crome	HDPE	Coban – Crome	Ti6Al4V
Material 2	PEEK	HDPE	25% CF – PEEK	25% CF – PEEK

Table -3: Material properties

Materials	Elastic Module E (MPa)	Poisson's Coefficient	Density (g/cm^3)	Yielding Stress (MPa)
Coban – Crome	210 000	0.29	8.28	420
HDPE	1070	0.41	0.955	21
Ti6Al4V	110 000	0.29	4.45	880
PEEK	3760	0.3779	1.35	65
25% CF – PEEK	17 000	0.3779	1.35	112

2.2 Analysis of human activities

In this study, we will analyze the various active postures of the patient to understand how force impacts the hip joint in those positions. The patient's everyday active postures to be examined include normal walking, sitting on a chair, and sitting on the ground. The rotation angles of the hip joint will change with each posture, and these rotation angles are illustrated in the Figure 2.

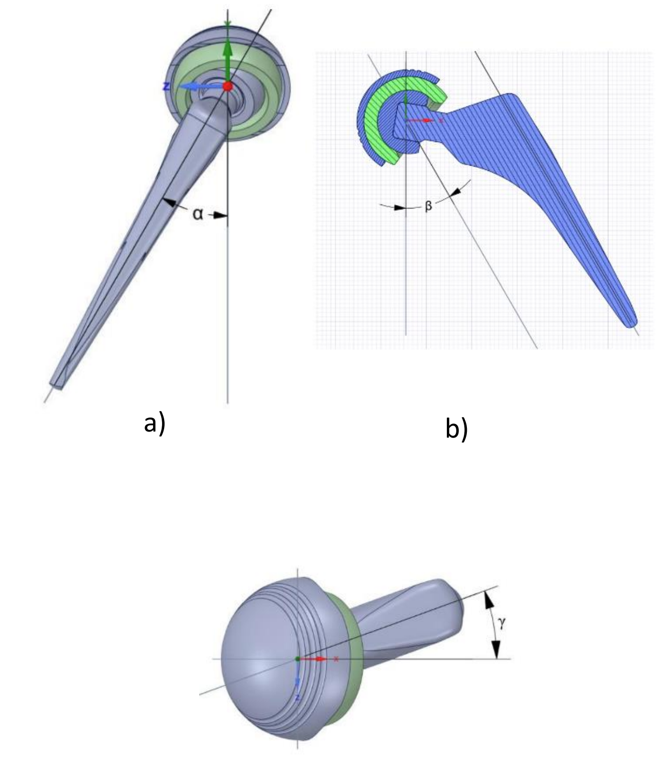

a) b) c)

Figure -2: Define the hip joint angles

The angles of hip joint rotation include three rotation angles around three axes (Fig.2): swinging the leg forward and backward (flexion and extension), moving the leg outward and inward (abduction and adduction), and rotating the leg around the joint (external and internal rotation). In normal walking, you have standing, moving forward, and moving backward. When sitting on a chair, you have the postures of picking up an object, getting up from the chair, and sitting down. When sitting on the ground, you can bow with your legs fully flexed at the knee, squat, and kneel. The values of the rotation angles of the hip joint in each posture are listed in Table 4. In which sitting postures have larger joint movement angles than normal walking postures.

Table -4: Hip joint angles for human activities [3], [9]

Human Activities	Flexion/ Extension (α)	Adduction/ Abduction (β)	Internal /External rotation (γ)
Walking			
Standing	0°	0°	0°
Forward	30°	0°	0°
Backward	-10°	0°	0°
Sit on the chair			
Picking up an object while sitting on the chair	86°	- 6,1°	- 12°
Getting up from the chair	76°	- 2.5°	- 11°
Sitting down on the chair	62°	- 0.92°	- 7
Sitting on the ground			
Bowing while sitting on legs fully flexed at the knee	84°	- 2.1°	- 12°
Squatting	80°	- 8.6°	- 9,2°
Kneeling	61°	- 1.2°	- 15°

2.2 Boundary and Loading conditions

The mechanical behavior of the present dual mobility hip joint will be investigated using the FEM method by Ansys software. Corresponding to each patient's posture is a corresponding set of hip joint degrees. Assuming the weight of the body and the weight carried is 3240N, the pressure on the Cup surface will be calculated as follows:

$$p = \frac{F}{S} = \frac{P \cos 50^0}{0.2772} = 0.765\ (Mpa)$$

Table -5: Coefficients of materials

Contacts	Materials	Fiction coefficient
Cup-liner	Coban-chrome/HDPE	0.1
Liner-Head	HDPE/ Ti6Al4V	0.1

The stem is press-fitted inside the femur so that a part of the stem will be fixed (Fig.3). The contact of the liner inside the cup and the head inside the liner will be considered friction contact. The coefficients of friction corresponding to the materials of the cup, head, and liner are given in table 5. The head is fixed with the stem.

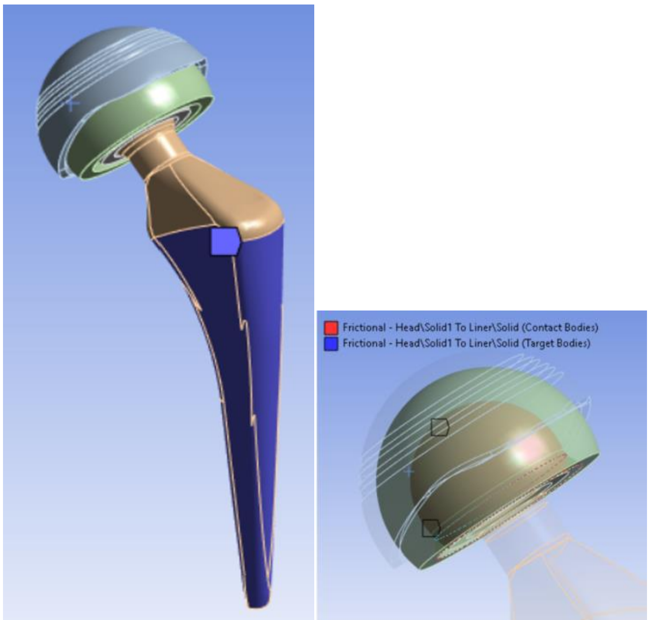

Figure -3: Boundary conditions of the AHJ

2.4 Convergency method

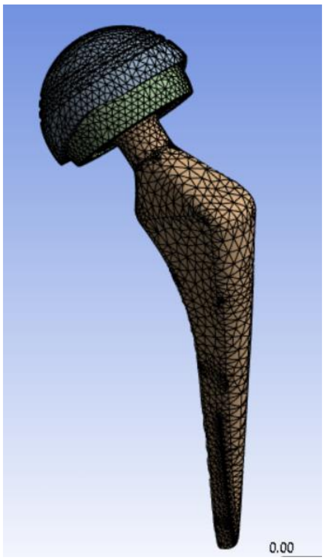

Figure - 4: The finite element meshing of the AHJ

After setting the boundary conditions and applying the force to the implant, the meshing step will be performed with an initial mesh size of 2mm, Tetra element type, with 24788 elements (Fig.4). To evaluate the convergence of the obtained results, the results of the Structure error analysis and the automatic convergence meshing are used. For example, when using the automatic convergence meshing to evaluate the convergence of the equivalent stress and the sliding distance on the stem part in the bowing position, the number of nodes increased from 44316 to 399299, which gave convergent results (Fig. 5)

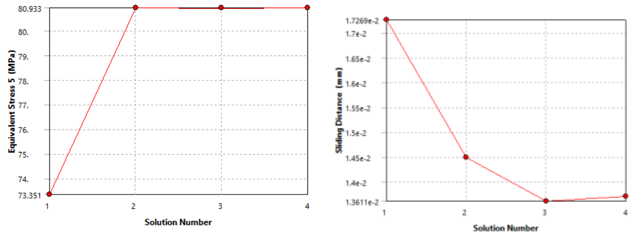

	Equivalent Stress 5 (MPa)	Change (%)	Nodes	Elements
1	73.351		44316	24851
2	80.932	9.8264	224341	143834
3	80.932	1.0725e-003	348187	231297
4	80.933	5.8e-004	398239	266491

	Sliding Distance (mm)	Change (%)	Nodes	Elements
1	1.7269e-002		44316	24851
2	1.4498e-002	-17.446	224341	143834
3	1.3611e-002	-6.3064	348187	231297
4	1.3703e-002	0.67079	398239	266491

Figure -5: The convergence results in the equivalent stress and the sliding distance

3. RESULTS AND DISCUSSIONS

3.1 The equivalent stress and total strain in the AHJ.

The results for Von-Mises equivalent stresses, maximum total deformations, and maximum total strains in the implants for each position, with group of Material 1 are provided in Tables 6 to 8. In all the cases examined, the highest stress was observed on the stem, followed by the cup and the head, with the lowest stress on the liner. Meanwhile, the largest deformation and displacement were mainly on the liner. It can be seen from the tables that sitting positions with a chair or sitting on the ground result in higher maximum stress (ranging from 65.591 MPa to 85.729 MPa) compared to the normal walking position (ranging from 32.602 MPa to 51.277 MPa). Among the sitting positions, bowing while sitting on legs fully flexed at the knee is the most dangerous, and among the walking positions, the forward has more stress on the stem, which is also a common movement posture of the patient. Total displacement and equivalent stress in the most dangerous case - bowing while sitting on legs fully flexed at the knee are given in detail in Figure 6 to Figure 15. The highest stress occurs at the front of the neck stem in all postures. The upper neck area bears the most force, while the lower area attached to the bone experiences less stress. As a result, when the patient walks, the stem doesn't put much force on the bone-joining position.

Next, we examine the mechanical behavior of the above hip joint made from a group of material 2 with the regular positions being standing and forward and the dangerous positions being bowing (Table 9). We see that the stress does not change much compared to the case of material 1, but the deformation and displacement increase relatively.

Table -6: Equivalent stresses, max total deformations and max total strains of AHJ in walking postures, Material 1

Parts	Von-mises Stresses (MPa)			Max Total Deformation (mm)			Max Total Strain		
	Standing	Forward	Backward	Standing	Forward	Backward	Standing	Forward	Backward
Cup	13.001	13.124	13.145	2.1007e-002	3.0572e-002	2.2417e-002	6.1911e-005	6.2495e-005	6.2598e-005
Liner	1.9314	1.9317	1.9454	2.4435e-002	3.3427e-002	2.5863e-002	1.8051e-003	1.8053e-003	1.8181e-003
Head	4.3878	4.5187	4.3383	8.3434e-003	1.7281e-002	9.7749e-003	2.0941e-005	2.1552e-005	2.07e-005
Stem	32.602	51.277	36.877	6.9336e-003	1.398e-002	8.0667e-003	2.9688e-004	4.6692e-004	3.3548e-004

Table -7: Equivalent stresses, max total deformation and max total strain of AHJ in sitting on chair postures, Material 1

Parts	Von-mises Stresses (MPa)			Max Total Deformation (mm)			Max Total Strain		
	Picking up an object	Getting up	Sitting down	Picking up an object	Getting up	Sitting down	Picking up an object	Getting up	Sitting down
Cup	12.927	13.235	13.199	4.4296e-002	4.5417e-002	4.3538e-002	6.1557e-005	6.3023e-005	6.2853e-005
Liner	1.9823	1.996	1.9311	4.5792e-002	4.6975e-002	4.5282e-002	1.8533e-003	1.8668e-003	1.8048e-003
Head	4.6845	4.9346	4.9114	2.7735e-002	2.8166e-002	2.7009e-002	2.2371e-005	2.3576e-005	2.3539e-005
Stem	80.933	81.61	76.351	2.2061e-002	2.2402e-002	2.1529e-002	7.3701e-004	7.4296e-004	6.9485e-004

Table -8: Equivalent stresses, max total deformation and max total strain of AHJ in sitting on ground postures, Material 1

Parts	Von-mises Stresses (MPa)			Max Total Deformation (mm)			Max Total Strain		
	Bowing	Squatting	Kneeling	Bowing	Squatting	Kneeling	Bowing	Squatting	Kneeling
Cup	12.991	13.059	12.739	4.6517e-002	4.3191e-002	3.3913e-002	6.1862e-005	6.2184e-005	6.0666e-005
Liner	1.8669	1.9307	1.805	4.7794e-002	4.485e-002	3.6018e-002	1.7448e-003	1.8044e-003	1.687e-003
Head	5.2104	4.7777	5.0562	2.9417e-002	2.6707e-002	2.1004e-002	2.6196e-005	2.2791e-005	2.4236e-005
Stem	85.729	74.893	65.591	2.3362e-002	2.1312e-002	1.6823e-002	7.8021e-004	6.8178e-004	5.969e-004

Table -9: Equivalent stresses, max total deformation and max total strain of AHJ in postures: standing, forward, and bowing while sitting on legs fully flexed at the knee, Material 2

Parts	Von-mises Stresses (MPa)			Max Total Deformation (mm)			Max Total Strain		
	Standing	Forward	Bowing	Standing	Forward	Bowing	Standing	Forward	Bowing
Cup	2.1223	2.1177	2.3596	7.7292e-002	0.14931	0.25065	5.6455e-004	2.1177	6.2757e-004
Liner	1.579	1.7219	2.5095	7.2872e-002	0.14026	0.23349	1.4802e-003	1.7219	2.3591e-003
Head	4.5807	3.5782	8.5002	5.3789e-002	0.11121	0.18917	2.7084e-004	3.5782	5.0327e-004
Stem	33.119	52.444	85.045	4.4504e-002	8.9877e-002	0.15003	1.9486e-003	52.444	5.0082e-003

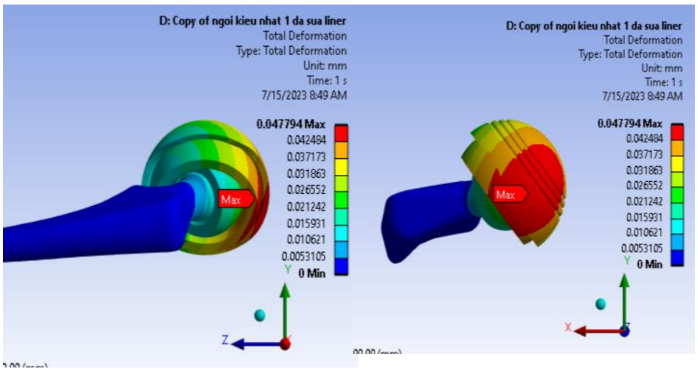

Figure -6: The total displacement distribution on the AHJ in Bowing while sitting on legs fully flexed at the knee position, Material 1

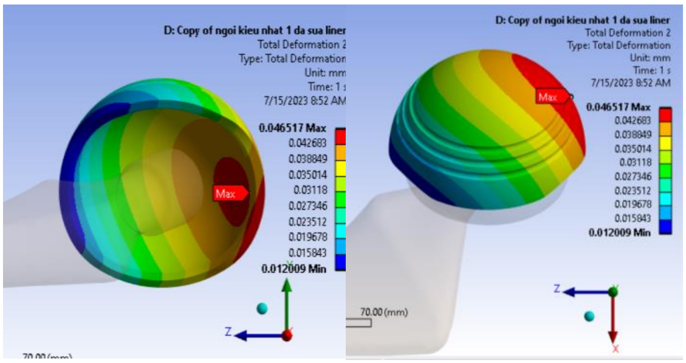

Figure -7: The total displacement distribution on the Cup in Bowing while sitting on legs fully flexed at the knee position, Material 1

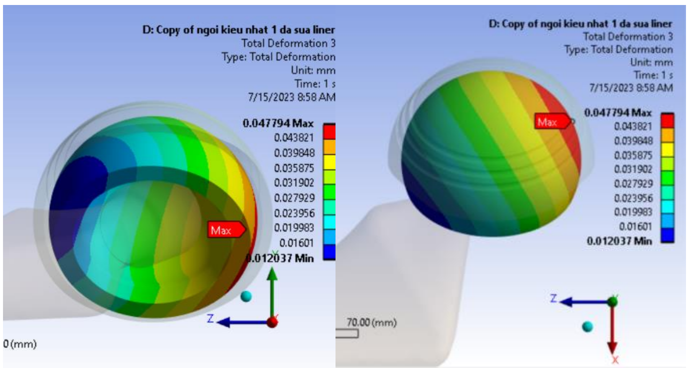

Figure -8: The total displacement distribution on the Liner in Bowing while sitting on legs fully flexed at the knee position, Material 1

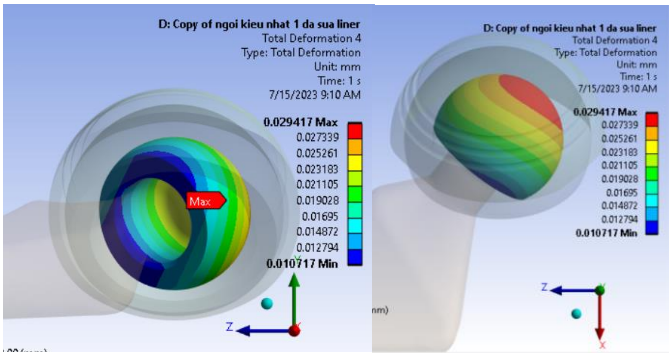

Figure -9: The total displacement distribution on the Head in Bowing while sitting on legs fully flexed at the knee position, Material 1

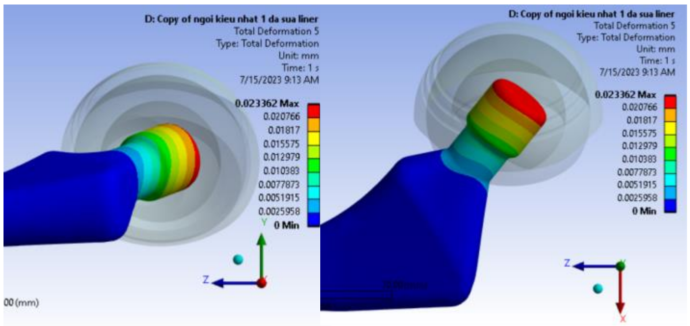

Figure -10: The total displacement distribution on the Stem in Bowing while sitting on legs fully flexed at the knee position, Material 1

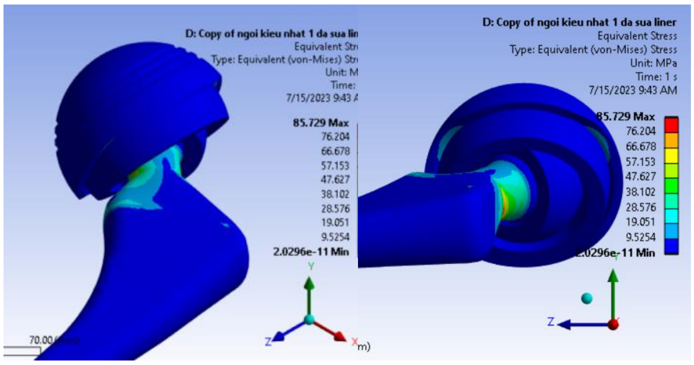

Figure -11: The equivalent stress distribution on the AHJ in Bowing while sitting on legs fully flexed at the knee position, Material 1

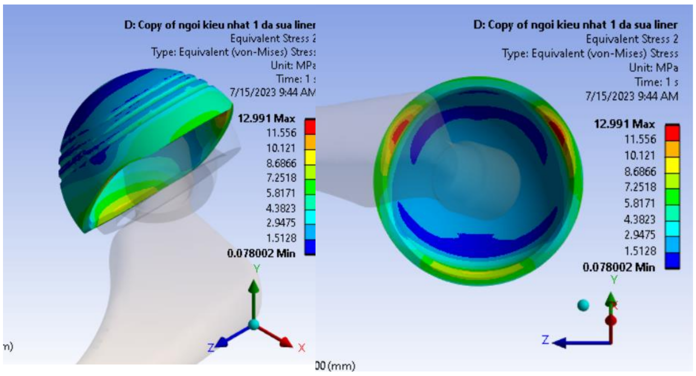

Figure -12: The equivalent stress distribution on the Cup in Bowing while sitting on legs fully flexed at the knee position, Material 1

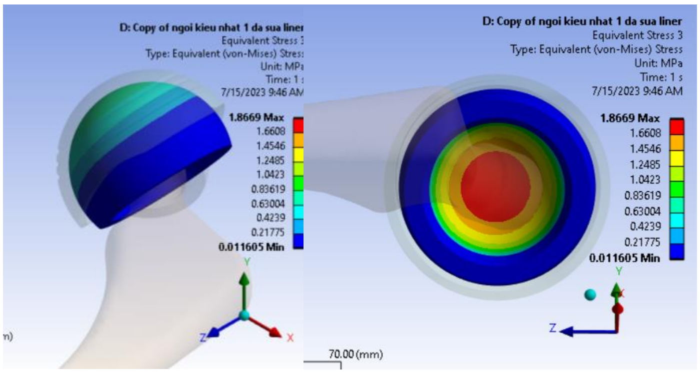

Figure -13: The equivalent stress distribution on the Liner in Bowing while sitting on legs fully flexed at the knee position, Material 1

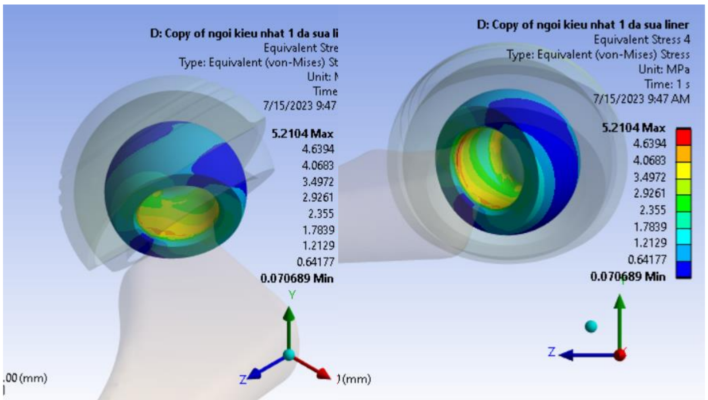

Figure 14: The equivalent stress distribution on the Head in Bowing while sitting on legs fully flexed at the knee position, Material 1

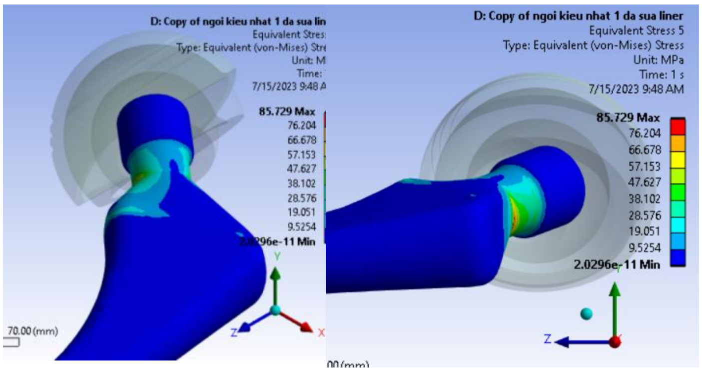

Figure -15: The equivalent stress distribution on the Stem in Bowing while sitting on legs fully flexed at the knee position, Material 1

3.2 Sliding Distance and Contact Pressure in the AHJ

In Table 10, it is observed that the highest contact pressure occurs at the Head and Stem, followed by the contact area between the Liner and Head. The Bowing and squatting positions exhibit the highest contact pressure between the Head and Stem (Figure 16). According to the results in Table 10, sliding distances primarily occur at the contact between the Liner and Head. The greatest sliding distances are observed during normal walking, squatting, sitting down, and sitting up shown in Figure 17. The sliding distance will impact the wear of the Liner and Head components during use, as the Liner material has a lower hardness than the Head material, resulting in wear primarily on the Liner (made of HDPE material), which is safe for the human body. According to the diagrams in Figures 16 and 17, the largest sliding distance occurs between the Liner and Head parts and is negligible at the Head and Stem connection. Therefore, even though the contact pressure at the Head and Stem is large, wear will mainly occur at the Liner and Head.

Table -10: The max contact pressure and sliding distance of AHJ in human activities, Material 1

	Cup – Liner Contact	Liner – Head Contact	Head – Stem Contact
Standing			
Contact Pressure	1.4827 MPa	2.321 MPa	6.0769 MPa
Sliding Distance	4.9552e-003 mm	1.4371e-002 mm	1.8734e-004 mm
Forward			
Contact Pressure	1.504 MPa	2.2583 MPa	6.305 MPa
Sliding Distance	4.9344e-003 mm	1.4406e-002 mm	2.0744e-004 mm

Backward			
Contact Pressure	1.4501 MPa	2.25 MPa	5.3502 MPa
Sliding Distance	4.9325e-003 mm	1.4472e-002 mm	1.955e-004 mm
Picking up an object while sitting on the chair			
Contact Pressure	1.5193 MPa	2.5277 MPa	6.1882 MPa
Sliding Distance	4.883e-003 mm	1.3703e-002 mm	3.0713e-004 mm
Getting up from the chair			
Contact Pressure	1.5013 MPa	2.4955 MPa	6.826 MPa
Sliding Distance	4.9784e-003 mm	1.447e-002 mm	2.9394e-004 mm
Sitting down on the chair			
Contact Pressure	1.5026 MPa	2.2562 MPa	6.9403 MPa
Sliding Distance	5.0055e-003 mm	1.4398e-002 mm	2.7177e-004 mm
Bowing while sitting on legs fully flexed at the knee			
Contact Pressure	1.5074 MPa	2.2398 MPa	8.4538 MPa
Sliding Distance	4.8843e-003 mm	1.3447e-002 mm	2.8268e-004 mm
Squating			
Contact Pressure	1.4961 MPa	2.261 MPa	7.2307 MPa
Sliding Distance	4.9303e-003 mm	1.4382e-002 mm	2.3311e-004 mm
Kneeling			
Contact Pressure	1.5443 MPa	2.6203 MPa	6.2834 MPa
Sliding Distance	4.6945e-003 mm	1.2164e-002 mm	2.6869e-004 mm

Table -11: The max contact pressure and sliding distance of AHJ in human activities, Material 2

	Contact Cup – Liner	Contact Liner – Head	Contact Head – Stem
Standing			
Contact Pressure	3.0684 MPa	1.8942 MPa	5.2947 MPa
Sliding Distance	3.2528e-003 mm	1.5766e-002 mm	1.4948e-003 mm
Forward			
Contact Pressure	3.8561 MPa	1.972 MPa	6.1776 MPa
Sliding Distance	3.6656e-003 mm	1.7484e-002 mm	1.7321e-003 mm
Bowing while sitting on legs fully flexed at the knee			
Contact Pressure	3.7691 MPa	4.4524 MPa	7.5319 MPa
Sliding Distance	3.6656e-003 mm	1.7484e-002 mm	1.7321e-003 mm

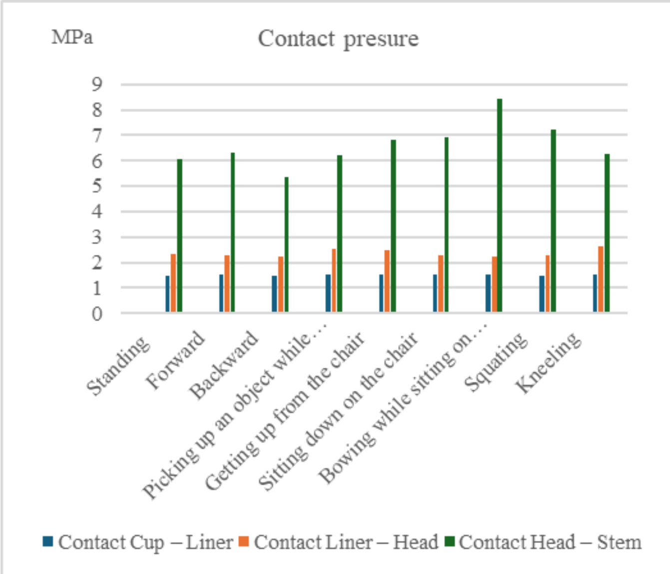

Figure -16: The max contact pressure in the AHJ, Material 1

In Material Group 2, the slipping distance between the Liner and Head is approximately 5-6% higher compared to Material Group 1, while that between the Liner and Cup of Material Group 2 is reduced by about 10% compared to Material Group 1 shown in Table 11.

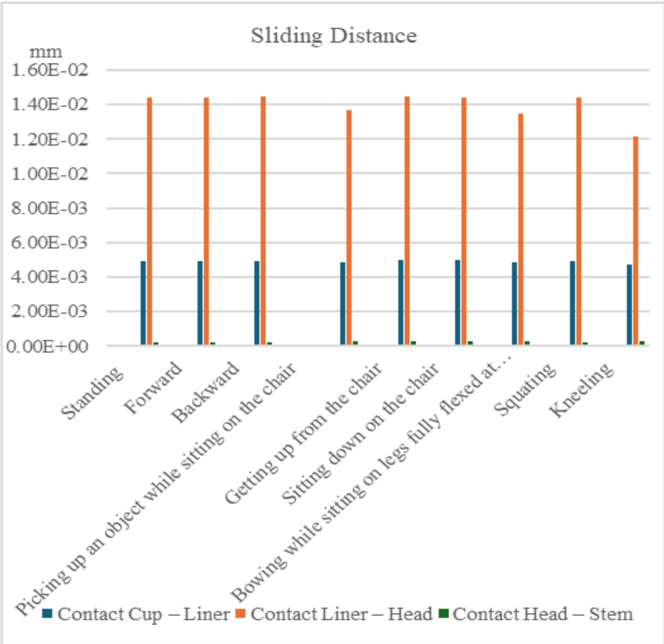

Figure -17: The max sliding distance in the AHJ, Material 1

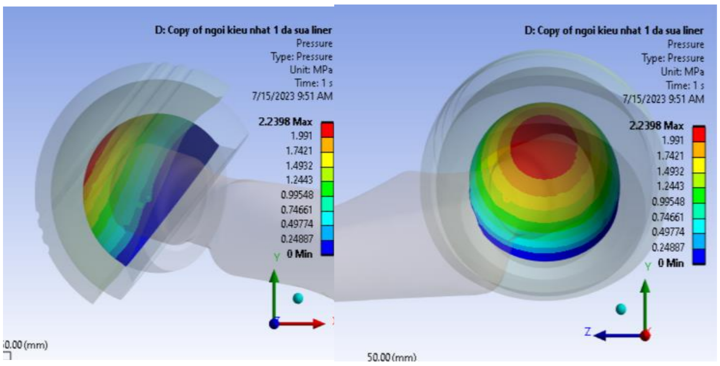

Figure -18: The contact pressure distribution between Liner-Cup in Bowing while sitting on legs fully flexed at the knee position, Material 1

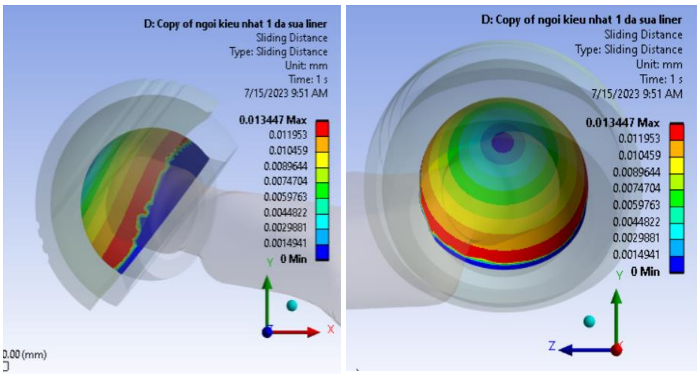

Figure -19: The sliding distance distribution between Liner-Cup in Bowing while sitting on legs fully flexed at the knee position, Material 1

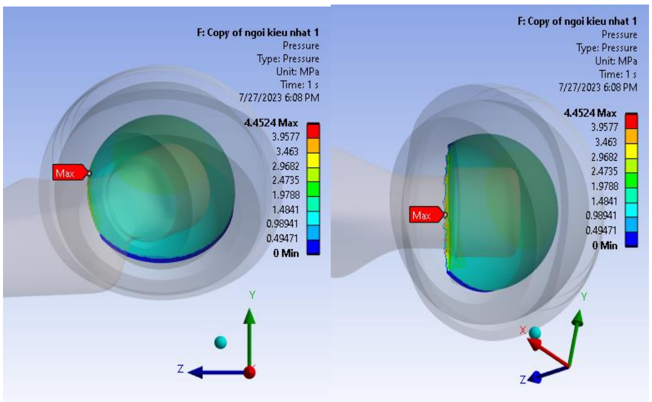

Figure -20: The contact pressure distribution between Liner-head in Bowing while sitting on legs fully flexed at the knee position, Material 2

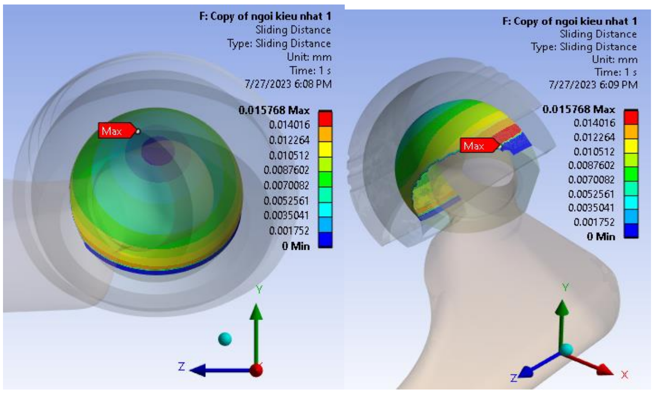

Figure -21: The sliding distance distribution between Liner-head in Bowing while sitting on legs fully flexed at the knee position, Material 2

From the distribution of contact pressure and sliding distance in the Cup and liner connection and the liner and head connection in Fig 18 to Fig 21, contact pressure and sliding distance have greater value in the outer rim on the liner and head contact.

4. CONCLUSION

This paper presents the mechanical behavior of the hip joint in the daily activities of the surveyed patients, including stress distribution, strain distribution, and displacement distribution on the dual mobility artificial hip joint components. The daily activities of the patients include normal walking postures (standing, forward, backward), sitting on a chair (picking up, getting up, getting down), and sitting on the ground without a chair (kneeling, bowing, squatting). These postures are suitable for the daily activities of an Asian patient in general and a Vietnamese patient in particular. From these results, it is possible to predict the patient's dangerous posture that should be avoided. The contact behavior between the hip joint components in all the above activities of the patient was also surveyed, including parameters of contact pressure and sliding distance. These parameters allow the prediction of joint slippage and wear during the patient's long-term activities.

ACKNOWLEDGEMENT

This research is funded by Hanoi University of Science and Technology (HUST) under project number T2022-PC-033.

REFERENCES

[1] Charles W. Radcliffe, "The Biomechanics of the Canadian-Type Hip Disarticulation Prosthesis", O&P Library Artificial Limbs, Vol 4, no 2, pp. 29-38 (1957).
[2] Derar, H. & Shahinpoor, M., "Recent Patents and Designs on Hip Replacement Prostheses", The Open Biomedical Engineering Journal, no. 9, pp.92–103 (2015).
[3] Eko Saputraa, Iwan Budiwan Anwara, J. Jamarib, Emile van der Heidea, "Finite Element Analysis of Artificial Hip Joint Movement during Human Activities", Proceeding Engineering, Vol 68, pp. 102-108 (2013).
[4] Fuziansyah Bachtar, Xian Chen, Toshiaki Hisada, "Finite element contact analysis of the hip joint", Med Bio Eng Comput, Vol 44, pp. 643–651 (2006).
[5] Green, D. S. & Schlegel, J., "A Polyaryletherketone Biomaterial for use in Medical", Engineering, Materials Science, Medicine (2006).
[6] K. Saika, "Design Analysis of the Bearing Component of the Hip joint Prosthesis to Improve Distribution of Forces and Frictional Wear", Faculty of Health, Engineering & Science, University of Southern Queensland (2016).
[7] Kurtz, S. M. & Devine, J. N., "Peek Biomaterials in Trauma, Orthopedic, and Spinal Implants", Biomaterials, vol 28 (32) (2007).
[8] McLaurin, C. A., "Hip disarticulation prosthesis, Report" No. 15, Prosthetic Services Centre, Department of Veterans Affairs, Toronto. Canada, (1954).
[9] Yousuf Jamal Mahboba, Mohsin Abdullah Al-Shammari, "Improving of artificial hip joint design by studying multiple angles of articulation between femoral head and acetabular line", International Journal of Energy and Environment, Vol 10, Issue 4, pp.195-210 (2019).

BIOGRAPHIES

Le Thi Bich Nam is a lecturer in the School of Mechanical Engineering in Hanoi University of Science and Technology. Her main research field includes the finite element method and the dynamic stiffness method in mechanical behavior of materials and structures.